Catalysis Communications 38 (2013) 16–20

Contents lists available at SciVerse ScienceDirect

Catalysis Communications

journal homepage: www.elsevier.com/locate/catcom

Short Communication

AgBr@Ag/TiO_2 core–shell composite with excellent visible light photocatalytic activity and hydrothermal stability

Rongfang Dong, Baozhu Tian *, Jinlong Zhang, Tingting Wang, Qingsong Tao, Shenyuan Bao, Fan Yang, Cuiyun Zeng

Key Lab for Advanced Materials and Institute of Fine Chemicals, East China University of Science and Technology, 130 Meilong Road, Shanghai, 200237, PR China

ARTICLE INFO

Article history:
Received 17 December 2012
Received in revised form 21 March 2013
Accepted 11 April 2013
Available online 17 April 2013

Keywords:
Silver bromide
Titanium dioxide
Core–shell structure
Photocatalytic degradation
Organic pollutants

ABSTRACT

AgBr@Ag/TiO_2 core–shell photocatalysts were fabricated by a facile green route. TiO_2 was uniformly coated on the surface of cubic AgBr, making AgBr@Ag/TiO_2 core–shell photocatalyst show excellent hydrothermal stability. Beneficial from that Ag nanoparticles and AgBr can respond to visible light and core–shell structure can effectively separate the photogenerated electrons and holes, AgBr@Ag/TiO_2 core–shell composites exhibited outstanding visible light photocatalytic activity for the degradation of acid orange 7. The activity of AgBr@Ag/TiO_2 is related to the thickness of TiO_2 shell, and the optimal shell thickness for obtaining the highest activity is 10 nm.

1. Introduction

Semiconductor photocatalysis has been considered to be a promising solution for the degradation of organic pollutants in waste water and air [1–3]. Amongst various semiconductor photocatalysts, titanium dioxide (TiO_2) has been widely investigated owing to its optical and electronic properties, nontoxicity, highly chemical stability, and low cost [4,5]. However, the practical applications of TiO_2 are still restrained because of its low efficiency in sunlight utilization and poor quantum efficiency [6]. Many strategies such as doping with metals [7] or nonmetals [8], anchoring organic sensitizers [9], semiconductor composite [10], and noble metal loading [11] have been employed to extend the photo-response of TiO_2 to the visible light region and enhance the quantum efficiency. Unfortunately, these efforts still cannot well meet the requirements of future environmental technologies driven by solar energy.

Noble metal nanoparticles (e.g., Au, Ag, Pt) exhibit strong visible-light absorption due to their surface plasmon resonance (SPR) [12]. Therefore, noble metal nanoparticles (NPs) have been employed as a kind of visible light harvestor to fabricate visible light-responsive photocatalysts [13]. Recently, silver halide-based plasmonic photocatalysts (denoted as AgX@Ag; X = Cl, Br) have received much attention due to their excellent visible-light photocatalytic activity for degrading organic pollutants [14–17]. Some researches proved that AgBr@Ag coupled with TiO_2 [18,19], Bi_2WO_6 [20], or other supports [21,22] usually show enhanced visible-light photocatalytic performance for organic pollutant degradation, which is beneficial from the effective separation of photogenerated carries [22]. For instance, Wang et al. [23] prepared mesoporous TiO_2 coated with Ag and AgBr nanoparticles, which exhibits high photocatalytic activity for MO degradation under visible light irradiation. However, for these hybrids, AgBr@Ag is always loaded on the surface of coupling materials and inevitably subjected to environmental corrosion, resulting in the deterioration of stability.

In the present work, we fabricated core–shell structural AgBr@Ag/TiO_2 photocatalysts via a facile green route, including controllable double-jet precipitation technique to synthesize uniform cubic AgBr core, precipitation method to coat TiO_2 shell, and UV light reduction to generate Ag NPs in the interface of AgBr and TiO_2. By fabricating this core–shell structure, the stability of AgBr can be effectively improved. The photocatalytic activities of the obtained samples were evaluated in terms of the degradation of acid orange 7 (AO7), methyl orange (MO), and 2,4-dichlorophen (2,4-DCP). Moreover, the degradation mechanism of organics over AgBr@Ag/TiO_2 was investigated by radical-trapping experiments.

2. Experimental

2.1. Synthesis of AgBr@Ag/TiO_2

Firstly, cubic AgBr grains were fabricated by controllable double-jet precipitation method (for details see Supplementary material). Then, TiO_2 shell was coated with the following processes: the pH of AgBr suspension was adjusted to 2 with dilute H_2SO_4 solution, and a desired

* Corresponding author. Tel./fax: +86 21 64252062.
E-mail address: baozhutian@ecust.edu.cn (B. Tian).

1566-7367/$ – see front matter © 2013 Elsevier B.V. All rights reserved.
http://dx.doi.org/10.1016/j.catcom.2013.04.006

amount of $Ti(SO_4)_2$ was added. Subsequently, the temperature of the suspension was slowly elevated to 80 °C. Then, the muddy liquid was transferred into a Teflon-inner-liner stainless autoclave and kept at 120 °C for 12 h. After the autoclave was cooled to room temperature, the sample was separated by centrifugation, washed with deionized water, and dried at room temperature. AgBr/TiO_2 samples with nominal shell thickness of 0.01, 0.02, 0.03, 0.04, and 0.05 μm were synthesized, and denoted as AgBr/TiO_2-0.01, AgBr/TiO_2-0.02, AgBr/TiO_2-0.03, AgBr/TiO_2-0.04, and AgBr/TiO_2-0.05, respectively. Pure TiO_2 was prepared with the same procedure in the absence of AgBr.

UV light reduction was employed to form Ag NPs. In a typical procedure, 0.5 g of AgBr/TiO_2 powder was put into a quartz tube containing 100 mL of water, and irradiated with a 150 W high-pressure Hg lamp ($\lambda_{max} = 365$ nm) for 2 h under stirring. Finally, AgBr@Ag/TiO_2 photocatalysts were obtained in sequence by centrifugation, washing, and drying. AgBr sample that only experienced UV light reduction was designated as AgBr@Ag, while the sample that experienced both hydrothermal treatment and light reduction was denoted as AgBr@Ag–H. For comparison, N-doped TiO_2 (N–TiO_2) was prepared according to Reference [24].

2.2. Characterization

The samples were characterized by scanning electron microscopy (SEM, JEOL JSM-6360 LV), X-ray diffractometer (XRD, Rigaku D/max 2550 VB/PC), X-ray photoelectron spectroscopy (XPS, Perkin-Elmer PHI 5000), and UV–vis–NIR spectrophotometer (SHIMADZU UV-2450) equipped with an integrating sphere assembly.

2.3. Photocatalytic activity test

Acid orange 7 (AO7), methyl orange (MO), and 2,4-dichlorophen (2,4-DCP) were selected as model pollutants to evaluate the photocatalytic activities of the obtained samples. The photocatalytic reaction was conducted under visible light by using a 500 W halogen tungsten lamp with a UV cut-off filter ($\lambda \geq 420$ nm). For each measurement, a specific amount of photocatalyst sample was added into a quartz tube containing 100 mL of 20 mg L^{-1} model pollutant aqueous solution (for details see Table S1). Prior to light irradiation, the suspension was stirred for 30 min in the dark to attain the adsorption–desorption equilibrium for model pollutant and dissolved oxygen on the surface of photocatalyst. At the given time interval, about 4 mL suspension was withdrawn, centrifuged, and filtered to remove the remaining particles. The residual concentrations of AO7 and MO were determined with a UV–Vis spectrophotometer, while the residual concentrations of phenol and 2,4-DCP were detected with a CTO-10 ASVP HPLC instrument. Total organic carbon (TOC) measurement was accomplished with a Shimadzu 5000A analyzer.

3. Results and discussion

Fig. 1(a–f) shows the SEM images of as-prepared AgBr, AgBr–H (after hydrothermal treatment), and AgBr/TiO_2 with different shell thicknesses. As shown in Fig. 1a, the obtained AgBr grains exhibited regular cubic morphology with side length of about 0.6 μm. After hydrothermal treatment, AgBr grains became irregular and aggregated, along with the growth of particle size (Fig. 1b). High temperature may accelerate the dissolution and regrowth of AgBr grains, resulting in the formation of irregular particles. This result indicated that AgBr grains are unstable in the hydrothermal circumstance. In contrast, the morphology of AgBr coated with TiO_2 shell kept unchanged after hydrothermal treatment (Fig. 1c–f), indicating that TiO_2 shell can effectively improve the hydrothermal stability of AgBr. When the nominal thickness of TiO_2 shell was below 0.02 μm, TiO_2 shell can be uniformly coated on AgBr core surface (Fig. 1c and d). Gradually, TiO_2 nanoparticles appeared when the nominal thickness of TiO_2 was increased to 0.03 μm. Finally, interconnected aggregates of TiO_2-wrapped AgBr grains were formed when the nominal thickness of TiO_2 was increased to 0.03 μm. The SEM image of AgBr@Ag/TiO_2-3 is shown in Fig. 1g, which indicated that UV light reduction does not change the morphological structure of AgBr/TiO_2. To observe the actual structure of TiO_2 shell, the AgBr core was removed by $Na_2S_2O_3$ aqueous solution. Fig. 1h shows that the TEM image of TiO_2 shell comes from AgBr/TiO_2-0.03, in which the cubic profile of AgBr grain remains visible.

The X-ray diffraction (XRD) patterns of the samples are shown in Fig. 2. All samples exhibited very approximate diffraction peaks at $2\theta = 26.7°$, 31.0°, 44.3°, 55.0°, 64.5°, and 73.3° (the left illustration of Fig. 2), which can be indexed to AgBr (111), (200), (220), (222), (400), (420) plane reflections (JCPDS file: 06-0438), respectively. The Y-coordinate was enlarged in the range of $2\theta = 24–26.5°$ and $2\theta = 36.5–39°$ (the right illustration of Fig. 2). All samples showed weak peaks around the scattering angle of $2\theta = 38.2°$, corresponding to Ag (111) diffraction peak (JCPDS file: 65-2871), while the weak peaks around $2\theta = 25.3°$ should be assigned to anatase (101) diffraction peak (JCPDS file: 21-1272). The intensity of anatase (101) diffraction peak gradually enhanced with the increase of nominal TiO_2 content, implying that the thickness of TiO_2 shell can be tuned by changing the addition amount of titanium precursor. In addition, the crystalline phase of TiO_2 prepared by the same hydrothermal process was also characterized by XRD and proved to be pure anatase phase (Fig. S1). The XPS spectra of the representative sample AgBr@

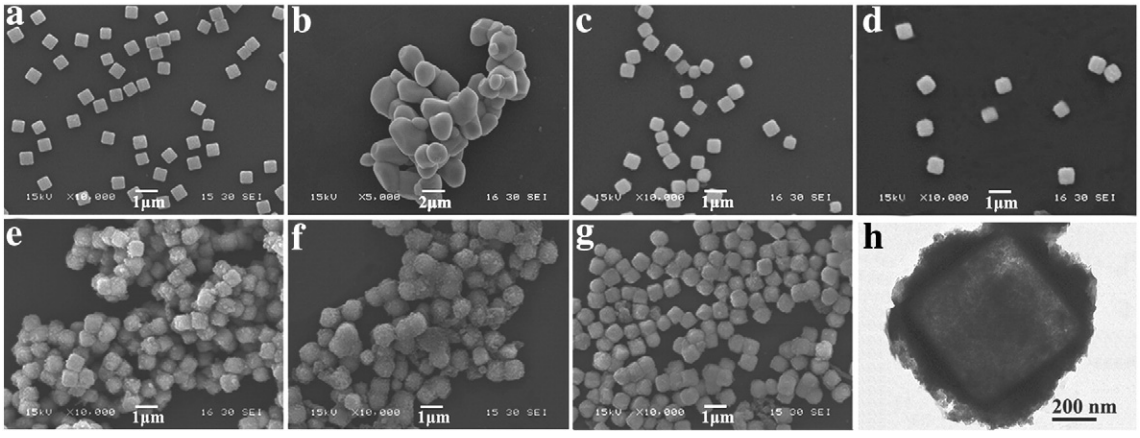

Fig. 1. SEM images of (a) As-prepared AgBr, (b) AgBr–H (after hydrothermal treatment), (c) AgBr/TiO_2-0.01, (d) AgBr/TiO_2-0.02, (e) AgBr/TiO_2-0.03, and (f) AgBr/TiO_2-0.05, (g) AgBr@Ag-TiO_2-0.03, (h) TEM image of TiO_2 shell from AgBr/TiO_2-0.03.